

The role of the Rashba coupling and domain wall bulging on dynamical induced electromotive force: A Berry curve investigation

N. Darmiani, T. Farajollahpour and A. Phirouznia

Department of Physics, Azarbaijan Shahid Madani University, 53714-161, Tabriz, Iran

Condensed Matter Computational Research Lab. Azarbaijan Shahid Madani University, 53714-161, Tabriz, Iran

(Dated: May 17, 2022)

A Berry curve investigation has been made on the magnetic modulated structures such as domain walls (DWs) and helimagnetic spin configurations. Results of the present study shows that the geometry of the spin configuration and the direction of the magnetic field creating the spin precession are of crucial importance in the magnitude of obtained electromotive force. It was also shown that the magnitude of the electromotive force decreases by increasing the Rashba coupling strength. In the previous researches in this field it was demonstrated that the rigid domain wall (DW) motion can not generate electromotive force in the system. In the current study it was demonstrated that this is not the case for a deformed DW and the DW bulging could be responsible for electromotive force of the rigid DW motion.

I. INTRODUCTION

During the last decades, a big effort has been devoted to the investigation of the magneto-resistive system. These investigations have been performed in the hope that the non-equilibrium charge and spin currents can be controlled by magnetic structure of the system. Modulation of the electric current in magnetic structures can be employed in new generation of electronic devices. One type of such systems, are known as giant magneto-resistive (GMR) structures have already used in the fabrication of new generation of hard-disk and read-heads¹⁻³. Among the magnetic structures very interesting transport properties have been reported for magnetic domain walls (DWs). It was shown that the magneto-resistance (MR) of a domain wall (DW) can be of either sign. In both type of theoretical and experimental works positive and negative MR has been reported for the DW⁴⁻⁹. Therefore transport in the DW has become a controversial dilemma which deserves some attention to understand the underlying physics of the charge transfer in magnetic modulated structures.

A central problem of spintronics research is the understanding the relation between the electronic transport and the dynamics of magnetic background. The presence of a DW changes the electrical resistance of a ferromagnetic conductor¹⁰⁻¹³.

The DW response to the external current could be investigated with another point of view in which the dynamics of DW and mutual effects between the domain and spin of carriers have been considered. It was reported that DWs could be driven at high electric currents. This effect can be considered as DW dynamics in the presence of spin torque generated by spin current. DW can be driven by spin-transfer process.

The possibility of the inverse of this effect has also been predicted by Berger in 1986 which known as ferro-Josephson effect¹⁴. In this effect an electromotive force (emf) has been generated by a moving DW. In recent years this effect has been reported experimentally.

Shenyang¹⁵ et.al, confirmed this theoretical prediction. They calculate theoretically and detect experimentally the electromotive force in a nano-strip induced by a moving magnetic DW. Their result showed that the electromotive force depends only on the topological nature of DW¹⁵. The result obtained by Berger have been reformulated by others via alternative approaches¹⁴⁻²¹. It was shown by Barends and Meekawa that the electromotive force is a spin Berry phase manifestation in the adiabatic transport¹⁶ round a closed loop. Numerical investigations demonstrate the existence of a spin-motive force acting on spin carriers in a precessing DW in which the spin-motive force has the same magnitude as the one described by Barnes and Maekawa²¹. Nonadiabatic corrections have been taken into account to determine the voltage generated by a field-driven transverse DW, for both the diffusive and ballistic regimes^{19,21}. Where the effects of anisotropic magnetoresistance on the induced voltage have been also considered. It was also shown that the ferro-Josephson effect could be explained by using a non-equilibrium thermodynamic approach¹⁷.

By using a local gauge-invariant formalism it was shown by Yang and et al that this electromotive force generation can be explained as a real space topological pumping effect²². Meanwhile they have demonstrated that the rigid translation of the DW without precession, which takes place when the DW driving magnetic field is less than the Walker breakdown²³, cannot induce electromotive force by the topological pumping. It was shown that the spin precession has the main role in generation of the electromotive force and even the precessing of pinned DWs could generate electromotive force along the system²².

In the present work we have employed the same approach when the inversion symmetry has been broken by the Rashba coupling. Calculations have been performed for different types of the magnetic modulated structures such as DWs and helimagnetic structures for both Néel-type and Bloch-type configurations. It was shown that the magnitude of the electromotive force in these structures can effectively been controlled by the Rashba coupling. It

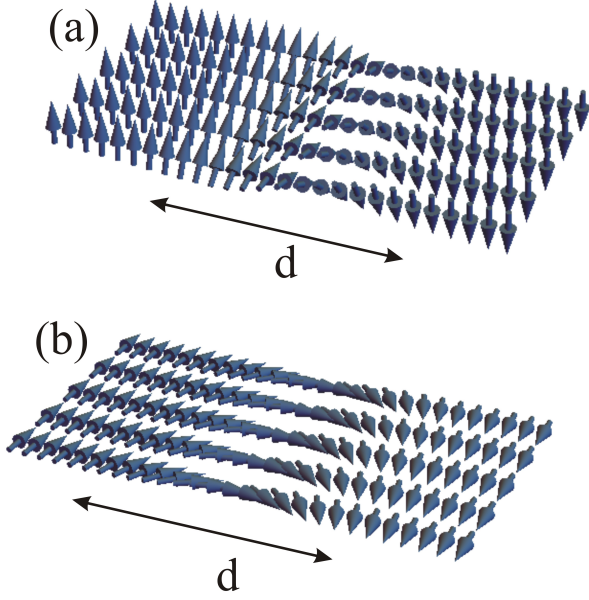


FIG. 1: The two-dimensional Bloch (a) and Néel-type (b) domain walls. Where d indicates the domain wall width

was also shown that for some special magnetic modulated structures, in which the k-space and real-space Berry curvatures expected to vanish identically, non-vanishing Berry curvatures could be induced by the Rashba coupling. Then we have obtained the influence of the DW bulging on real space topological pumping effect during the rigid DW motion. Results indicate that the rigid motion of a deformed DW could generate an effective electromotive force in the system.

In the present work two different profiles of magnetic configuration have been considered. First profile corresponds to a DW located between the oppositely directed ferromagnetic regions. The local direction of the magnetization inside the DW varies along the DW width. Second profile corresponds to a commensurate helimagnetic structure in which the magnetic unit cell is integer times of the chemical unit cell. These two profiles have been identified by the functionality of polar angle and azimuthal angles (ϕ, θ) of the localized spins in the spherical coordinate. Each of these profiles could be either Néel or Bloch type. For two-dimensional structures, when the rotation axis of the localized spins is normal to the plane containing the localized dipole atoms the structure known as Néel type magnetic orientation meanwhile when the rotation axis is in the plane of dipole atoms the structure known as Bloch type magnetic orientation. These profiles of the magnetic configurations maybe given by $\phi(x) = (\pi x/a_m), \theta = \pi/2$ and $\phi = \text{const}, \theta(x) = (\pi x/a_m)$ for Néel-type and Bloch-type helimagnetic configurations respectively. On the other hand Néel-type and Bloch-type DWs could be considered by the following profiles $\phi(x) = (\pi/2) \tanh(x/d), \theta = \pi/2$ and $\phi = \text{const}, \theta(x) = (\pi/2) \tanh(x/d)$ respectively.

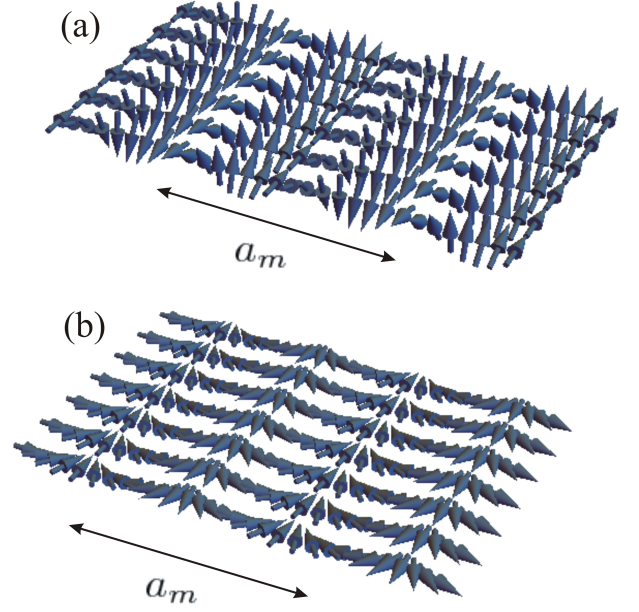


FIG. 2: The two-dimensional Bloch (a) and Néel-type (b) helimagnetic structures. Where a_m indicates the length of the magnetic unit cell

Here a_m is the lattice constant of the magnetic unit cell and d is the DW width. These magnetic configurations have been illustrated in Figs. 1 and 2. In the current work we have obtained an electromotive force for a DW and a helimagnetic structure in either of Néel or Bloch types of spin orientation. Results show that the electromotive force dependence on the direction of the magnetic field generating the precession and the spin configuration itself.

II. GEOMETRICAL BERRY APPROACH

The recent applications of Berry curvature in condensed matter physics and observation of elegant conclusions is a motivation for some calculations in DW studies. In 1984 Berry²⁴ pointed out that when the system undergoes an adiabatic change, a phase shift could be generated which may have observable consequences. The system will stay at one of the instantaneous eigenstates if the instantaneous state is well separated with the others and the time evolution is very slow (adiabatic evolution of the system is necessary). The first experimental verification of Berry phase is due to Tomita and Chio²⁵. A natural place to find the Berry phase is in the spintronics i.e. in the spin transport process. Where numerous researches that related to this topic can be found in literatures^{26–28}. Different terms of Berry curvature such as $\Omega_{kk}, \Omega_{kt}, \Omega_{rr}, \Omega_{kr}$ and Ω_{rt} provide different types of physical information each of them represents or measures an especial physical effect in condensed matter physics. The

k -space Berry curvature, Ω_{kk} , leads to an anomalous velocity which results in modification of the semiclassical equations. The anomalous Hall and spin Hall effects are originate from this anomalous velocity^{29–33}. When the system depends on certain time varying parameters, Ω_{kt} measures the charge pumping in the system^{34,35}. As an example, by consideration the simplest case of band insulator with a single fully occupied band along the x axis, if some parameters of the system periodically vary in time, then quantized charge can be pumped through the system over one period T , this results in quantization of charge in an integer multiple of first Chern number³⁶. Bird and et al showed that the Berry phase related to Ω_{rr} , can measure the electron diffraction pattern of deformed crystal³⁷. Meanwhile the surface integral of Berry curvature $\Omega_{x,y}$ of a vortex, gives a topological invariant known as *skyrmion* charge³⁸. It was shown that Liouville's conservation theorem of phase-space volume is violated by Berry curve considerations in the presence of a magnetic field. This violation results in modification of density of states where Ω_{kr} contributes in determination of this correction³⁹.

III. MODEL

In the current study the considered system is a magnetic two dimensional electron gas (2DEG) structure which contains one of the two possible types of chiral spin modulated configurations i.e. the DW spin structure or the helimagnetic spin arrangement. The general Hamiltonian which describes the electron inside these type of systems, in the presence of the Rashba coupling, could be expressed as

$$H = H_0 + H_{ex} + H_R. \quad (1)$$

Where

$$H_0 = \frac{-\hbar^2 \nabla^2}{2m} + V(r), \quad (2)$$

in which $V(r)$ is the lattice periodic potential, and the exchange between the localized magnetic moments and the conduction electrons, is expressed as

$$H_{ex} = J \hat{\sigma} \cdot \hat{n}(\vec{r}). \quad (3)$$

In the above relation, J is the exchange interaction strength, σ denotes the operator of spin in terms of the Pauli spin matrices and the unit vector $\hat{n}(\vec{r}) = \sin \theta \cos \phi \hat{x} + \sin \theta \sin \phi \hat{y} + \cos \theta \hat{z}$ is along the direction of local magnetization. The Rashba interaction is given by

$$H_R = \frac{\alpha}{\hbar} \hat{\sigma} \times \vec{P} \cdot \hat{z}, \quad (4)$$

where α is the Rashba coupling strength. The Rashba Hamiltonian commutes with the momentum operator and therefore could not be considered as

a scattering source in collinear spin structures. However the Rashba interaction could be considered as a spin relaxation mechanism in non-collinear spin configurations and magnetic modulated structures such as DW. It was shown that increasing the Rashba coupling strength could effectively increase the magnetoresistance in sharp DWs⁴⁰.

When an impurity free Hamiltonian is selected to describe the system properties. The DW pinning and magneto-resistive effects of these spin modulated structures have been automatically ignored. However as we will discuss about it later if we precession of a pinned DW results in electromotive force in the system. The Hamiltonian of the system can be expressed in the general form of the two-level systems as follows

$$H = H_0 + \vec{h}(\mathbf{R}) \cdot \hat{\sigma}, \quad (5)$$

where we have defined

$$\vec{h}(\mathbf{R}) = (Jn_x(\theta, \phi) + \alpha k_y) \hat{x} + (Jn_y(\theta, \phi) - \alpha k_x) \hat{y} + Jn_z(\theta, \phi) \hat{z}, \quad (6)$$

$\vec{h}(\mathbf{R})$ could be considered as a effective magnetic field of a spin dependent two-level system. Hamiltonian of the system has been given in term of some parameters identified by \mathbf{R} in which each of these parameters describing the adiabatic evolution of the system in the parametric space.

The spatial orientation of $h(\mathbf{R})$ could be a specified by the spherical angles given by

$$\begin{aligned} \cos \gamma &= \frac{h_z(\mathbf{R})}{|\vec{h}(\mathbf{R})|} \\ \beta &= \tan^{-1} \frac{h_y(\mathbf{R})}{h_x(\mathbf{R})}. \end{aligned} \quad (7)$$

In which in the present case one can obtain

$$\cos \gamma = \frac{Jn_z(\theta, \phi)}{\sqrt{J^2 + \alpha^2 k^2 + 2\alpha J(\hat{n} \times \vec{k})_z}} \quad (8)$$

$$\beta = \tan^{-1} \left(\frac{Jn_y(\theta, \phi) - \alpha k_x}{Jn_x(\theta, \phi) + \alpha k_y} \right). \quad (9)$$

Then the elements of Berry curvature in the parametric space are given by

$$\Omega_{R_i R_j} = \frac{1}{2} \frac{\partial(\beta, \cos \gamma)}{\partial(R_i, R_j)} = \frac{1}{2} \det \begin{pmatrix} \partial \beta / \partial R_1 & \partial \cos \gamma / \partial R_1 \\ \partial \beta / \partial R_2 & \partial \cos \gamma / \partial R_2 \end{pmatrix}. \quad (10)$$

IV. STATIC LIMIT

A. NÉEL TYPE SPIN CONFIGURATIONS IN THE STATIC LIMIT

At the static limit in the absence of the spin precession ($\omega \rightarrow 0$). By considering the effect of the Rashba

interaction for a Néel type two-dimensional helimagnetic structure the effective magnetic field of this two band system reads

$$\vec{h}_{NH}(R) = (J \cos(\frac{\pi x}{a_m}) + \alpha k_y)\hat{x} + (J \sin(\frac{\pi x}{a_m}) - \alpha k_x)\hat{y} \quad (11)$$

where the spin configuration profile is given by $\phi(x) = \frac{\pi x}{a_m}$, $\theta = \frac{\pi}{2}$. In this case the linear functionality of the polar angle provides a spin-periodic structure i.e. a helimagnetic configuration.

Then one can obtain $\cos \gamma = 0$. Therefore it can be shown that the Berry curvatures of Néel type Helimagnetic structure vanishes identically:

$$\Omega_{k_x k_y} = \Omega_{k_x x} = \Omega_{k_y x} = 0. \quad (12)$$

For a Néel type DW in the static limit the orientation profile is as follows: $\theta = \frac{\pi}{2}$ and $\phi = (\pi/2) \tanh \frac{x}{d}$. Where the local direction of the magnetization is given by $\hat{n} = \cos(\frac{\pi}{2} \tanh \frac{x}{d})\hat{x} + \sin(\frac{\pi}{2} \tanh \frac{x}{d})\hat{y}$. In this case the effective magnetic field is as follows

$$\begin{aligned} \vec{h}_{ND} = & (J \cos(\frac{\pi}{2} \tanh \frac{x}{d}) + \alpha k_y)\hat{x} \\ & + (J \sin(\frac{\pi}{2} \tanh \frac{x}{d}) - \alpha k_x)\hat{y}. \end{aligned} \quad (13)$$

Since h_{ND} is identified by the following orientation angles,

$$\cos \gamma = 0 \quad (14)$$

$$\beta = \tan^{-1} \left(\frac{J \sin(\frac{\pi}{2} \tanh \frac{x}{d}) - \alpha k_x}{J \cos(\frac{\pi}{2} \tanh \frac{x}{d}) + \alpha k_y} \right). \quad (15)$$

Similarly it can be easily shown that the Berry curvature of Néel type of DW in the presence of Rashba term, is zero.

$$\Omega_{k_x k_y} = \Omega_{k_x x} = \Omega_{k_y x} = 0. \quad (16)$$

In the other words the Berry curvature of the Néel type structures in the static limit always vanish. This can be simply obtained if we consider that the Berry curvature of any in plane effective magnetic field where $\cos \gamma = 0$ vanishes as a result of the Eq. (10). It should be noted that this result is independent of the spatial functionality of θ and ϕ which was assumed for each of these angles. Therefore while the effective magnetic field remains in the plane of the two dimensional spin texture the Berry curvature vanishes.

B. BLOCH TYPE SPIN CONFIGURATIONS IN THE STATIC LIMIT

For a two-dimensional Bloch type helimagnetic spin configuration at the static limit the local direction of the magnetization is given by $\vec{n} = \sin(\frac{\pi x}{a_m})\hat{y} + \cos(\frac{\pi x}{a_m})\hat{z}$ where

$\theta = \frac{\pi x}{a_m}$ and $\phi = \frac{\pi}{2}$, after some calculation the Berry curvature of system can be obtained.

$$\Omega_{k_x k_y} = \frac{1}{2} \frac{J \alpha^2 \cos(\frac{\pi x}{a_m})}{|\vec{h}_{BH}|^3} \quad (17)$$

$$\Omega_{k_x x} = \frac{1}{2} \frac{J \pi \alpha^2 k_y \sin(\frac{\pi x}{a_m})}{d |\vec{h}_{BH}|^3} \quad (18)$$

$$\Omega_{k_y x} = \frac{1}{2} \frac{J \pi \alpha (J - \alpha k_x \sin(\frac{\pi x}{a_m}))}{d |\vec{h}_{BH}|^3}, \quad (19)$$

where \vec{h}_{BH} stands for effective magnetic field for a Bloch type helimagnetic system which is given as follows

$$\vec{h}_{BH} = (\alpha k_y)\hat{x} + (J \sin(\frac{\pi x}{a_m}) - \alpha k_x)\hat{y} + (J \cos(\frac{\pi x}{a_m}))\hat{z}. \quad (20)$$

For a Bloch type magnetic DW the orientation of the local magnetization has been specified by the following profiles of the spherical angles i.e. $\theta = \frac{\pi}{2} \tanh \frac{x}{d}$ and $\phi = \frac{\pi}{2}$ are the assumptions. The effective magnetic field is

$$\begin{aligned} \vec{h}_{BD}(R) = & (\alpha k_y)\hat{x} + (J \sin(\frac{\pi}{2} \tanh \frac{x}{d}) - \alpha k_x)\hat{y} \\ & + (J \cos(\frac{\pi}{2} \tanh \frac{x}{d}))\hat{z} \end{aligned} \quad (21)$$

and therefore

$$\begin{aligned} \cos \gamma = & \frac{J \cos(\pi/2 \tanh \frac{x}{d})}{\sqrt{\alpha^2 k^2 - 2J \alpha k_x \sin(\pi/2 \tanh \frac{x}{d}) + J^2}} \\ \beta = & \tan^{-1} \left(\frac{J \sin(\pi/2 \tanh(x/d)) - \alpha k_x}{\alpha k_y} \right). \end{aligned} \quad (22)$$

So the Berry curvatures of the Bloch type of magnetic DW are given as

$$\Omega_{k_x, k_y} = \frac{1}{2} \frac{J \alpha^2 \cos(\frac{\pi}{2} \tanh \frac{x}{d})}{|\vec{h}_{BD}|^3} \quad (23)$$

$$\Omega_{k_x, x} = \frac{J \pi \alpha^2 k_y (1 + \tanh^2(\frac{x}{d})) \sin(\frac{\pi}{2} \tanh \frac{x}{d})}{4d |\vec{h}_{BD}|^3} \quad (24)$$

$$\Omega_{k_y, x} = \frac{J \pi \alpha (1 + \tanh^2(\frac{x}{d})) (J - \alpha k_x \sin(\frac{\pi}{2} \tanh \frac{x}{d}))}{4d |\vec{h}_{BD}|^3}. \quad (25)$$

Results indicate that the presence of the Rashba coupling has a central role in emergence of the k-space and

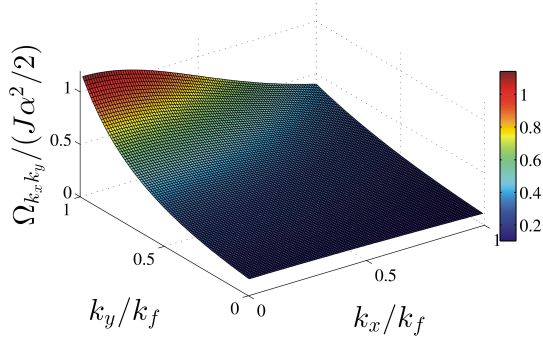


FIG. 3: K-space Berry curvature of a Bloch-type DW where $J = 0.1\epsilon_F$ and $\alpha = 0.5\epsilon_F/k_F$.

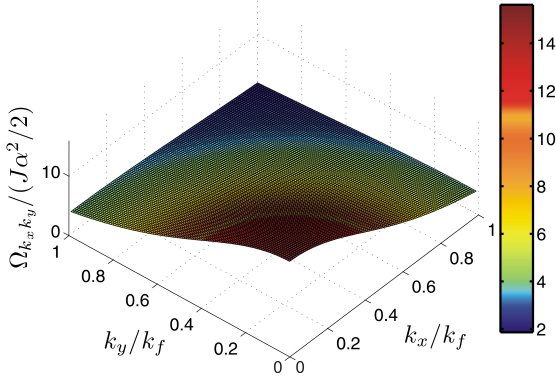


FIG. 4: K-space Berry curvature of a Bloch-type helimagnetic configuration where $J = 0.1\epsilon_F$ and $\alpha = 0.5\epsilon_F/k_F$.

phase-space Berry curves in Bloch type magnetic configurations. It can be easily shown that in the absence of the Rashba coupling these Berry curvatures identically vanish. Meanwhile it should be noted that at a typical fixed point in phase-space Berry curvatures are not monotonic functions of the Rashba coupling strength. Berry curvatures have been suppressed at high Rashba couplings where we have $\Omega_{ss'} \sim 1/\alpha$ in which s and s' are k_i and r_j . Obtained results of the k-space Berry curvature have been summarized in Figs. 3 and 4. Since the Hall conductivity is given by the following expression

$$\sigma_{xy} = \frac{e^2}{\hbar} \int_{BZ} \frac{d^2k}{(2\pi)^2} \Omega_{k_x, k_y}. \quad (26)$$

Results depicted in Figs. 3 and 4 indicate anisotropic contribution of different k-states in Hall conductivity in the DW. However this contribution could be considered quite isotropic in the helimagnetic structure. This anisotropy in the DW Berry curvature is the direct consequence of the breakdown of the periodic symmetry along x direction. Meanwhile it can be inferred that the states contributing in the Hall conductivity of a helimagnetic structure are located in the region of high wavelength limit.

V. PRECESSION INDUCED ELECTROMOTIVE FORCE AT LOW MAGNETIC FIELD

In the presence of the magnetic field, local magnetic moments start to precess about the direction of the field. Therefore the orientation of a localized magnetic moment (the local direction of the spin texture: \hat{n}) varies in space and time. This precession characterizes by the Larmor frequency, ω_L and \hat{n}_m which represents the rotation axis of the precession. In the adiabatic regime when \hbar/J , $1/\omega_L \ll l_m/v_F$, where l_m is the length scale in which the local magnetization changes and v_F is the Fermi velocity of the electrons, the spin of moving electrons will always be directed along the local direction of magnetization i.e. the moving spins obey the local spin direction during their motion. In this case electrons acquire Berry phase induced by localized spins. Provided that the above condition is satisfied one can obtain the space-time Berry curve, Ω_{xt} , which measures the induced electromotive force per unit length. Space-time Berry curve (Ω_{xt}) acts on the electrons like an effective electric field. The general formula for electromotive force by means of Berry curvature is defined as

$$emf = \frac{-\hbar}{e} \int dx \Omega_{xt}. \quad (27)$$

The spin precession induced by a normal magnetic field could be expressed by the following profiles for helimagnetic and DW spin configurations.

In these given profiles the magnetic field is assumed to be directed vertically to the two-dimensional plane of the system. For any arbitrary direction of the magnetic field space-time Berry curve could be obtained by straightforward but somewhat tedious calculations.

It should be noted that DW motion requires that the magnetic field overcome the impurity pinning potential in which the DW has been captured. Pinning of the DW arises due to the impurities and it was demonstrated that the precessing spins of a DW at rest results in effective electromotive force²². Meanwhile it should be noted that the motion of the Néel type DWs requires an in plane magnetic field greater than the depinning field. As mentioned before it was expected that the DW motion results in electromotive force along the magnetic system. However in the work described in Ref. 22 it was shown that the electromotive force generated by the DW is directly proportional to the precession frequency and the DW motion itself has not any contribution in the generated electromotive force. Therefore a pinned DW could also produce electromotive force while the DW is at rest and the local spins are precessing. This effect can take place when the magnetic field is less than the depinning field.

The enlargement of the magnetic domain, in the presence of the parallel magnetic field, manifests itself as motion of domain's boundary i.e. the DW movement. It can be inferred that the motion of the Néel type DWs requires an in plane magnetic field meanwhile the motion

of the Bloch type DWs could be generated by a normal field. However low field precession of spins cannot result in domain enlargement or DW motion when the normal magnetic field is less than the depinning field.

It can be simply shown that for both of the Néel type structures i.e. the Néel type DW and the Néel type helimagnetic system, space-time Berry curve ($\Omega_{x,t}$) vanishes identically. Therefore it could be inferred that the electromotive force vanishes when the direction of precession vector is identical with the rotation angle of the spin texture i.e. when $\hat{n}_D(r) \cdot \hat{n}_m = 1$ (or when $\hat{n}(r, t) \cdot \hat{n}_m = 0$) in which $\hat{n}_D(r, t)$ denotes the rotation axis of the magnetic modulated structure. In this case the precession cannot induce out of plane spin component and therefore $\cos(\gamma) = 0$ which indicates that

$$\Omega_{xt} = \frac{1}{2} \frac{\partial(\beta, \cos \gamma)}{\partial(x, t)}, = 0, \quad (28)$$

accordingly this results in $emf = 0$. However it can be easily shown that the space-time Berry curve does not

go all the way to zero for Néel type configurations when the applied magnetic field is not identical with the static spin the rotation axis.

In the presence of a normal field, the precession of the Bloch-type helimagnetic and DW configurations could be given by the following profiles $\phi = \omega t, \theta(x) = \pi(x/a_m)$ $\phi = \omega t, \theta(x) = (\pi/2) \tanh(x/d)$ respectively. Then for a Bloch type helimagnetic structure the effective magnetic field of the system can be given by the following expression

$$\begin{aligned} \vec{h}(x, t) = & (J \sin(\frac{\pi x}{a_m}) \cos(\omega t) + \alpha k_y) \hat{x} \\ & + (J \sin(\frac{\pi x}{a_m}) \sin(\omega t) - \alpha k_x) \hat{y} + J \cos(\frac{\pi x}{a_m}) \hat{z}. \end{aligned} \quad (29)$$

Then one can obtain the space-time Berry curve as follows

$$\Omega_{xt} = \frac{\pi \omega \left(\Lambda_k^{(1)}(\theta, \phi) |h_{BH}(\theta, \phi)|^2 + J^3 \sin(\theta) \cos^2(\theta) \Lambda_k^{(2)}(\theta, \phi) \right)}{2d \Lambda_k^{(3)}(\theta, \phi) |h_{BH}(\theta, \phi)|^3}. \quad (30)$$

Where we have defined

$$\begin{aligned} \chi_k(\phi) &= k_y \cos(\phi) - k_x \sin(\phi) \\ \Lambda_k^{(1)}(\theta, \phi) &= J^3 \sin^3(\theta) + \alpha J^2 \sin^2(\theta) \chi_k(\phi) \\ \Lambda_k^{(2)}(\theta, \phi) &= \alpha J \sin(\theta) \chi_k(\phi) + \alpha^2 k^2 \\ \Lambda_k^{(3)}(\theta, \phi) &= \alpha^2 k^2 + 2\alpha J \sin(\theta) \chi_k(\phi) + J^2 \sin^2(\theta). \end{aligned} \quad (31)$$

Similarly for a Bloch type DW in which space-time distri-

bution of the effective magnetic field could be considered as

$$\begin{aligned} \vec{h}(x, t) = & (J \sin(\frac{\pi}{2} \tanh(\frac{x}{d})) \cos(\omega t) + \alpha k_y) \hat{x} \\ & + (J \sin(\frac{\pi}{2} \tanh(\frac{x}{d})) \sin(\omega t) - \alpha k_x) \hat{y} \\ & + J \cos(\frac{\pi}{2} \tanh(\frac{x}{d})) \hat{z}, \end{aligned} \quad (32)$$

one can write

$$\Omega_{xt} = (1 + \tanh^2(x/d)) \frac{\pi \omega \left(\Lambda_k^{(1)}(\theta, \phi) |h_{BD}(\theta, \phi)|^2 + J^3 \sin(\theta) \cos^2(\theta) \Lambda_k^{(2)}(\theta, \phi) \right)}{4d \Lambda_k^{(3)}(\theta, \phi) |h_{BD}(\theta, \phi)|^3}, \quad (33)$$

Eqs. 30 and 33 indicate that the electromotive force switches off in the absence of the spin precession ($\omega = 0$) in both of the Bloch-type configurations. This means that the rigid DW motion could not generate electromotive force in the system as described in 22. Meanwhile it can be inferred from the Figs 5 and 6 that the precession induced electromotive force decreases by increasing the

Rashba coupling in the system.

Since the space and time dependence of β and $\cos \gamma$ are just through the dependence of the spherical angles (θ and ϕ). If we consider the problem in a general its form,

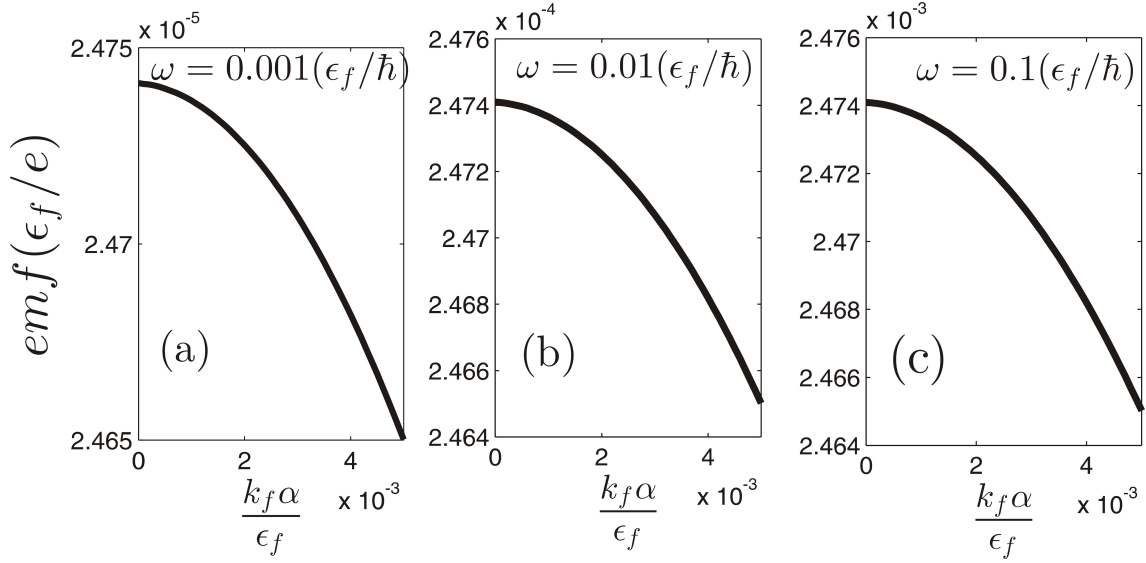


FIG. 5: The electromotive force induced in a Bloch type helimagnetic structure at different precession frequencies as a function of the Rashba coupling strength.

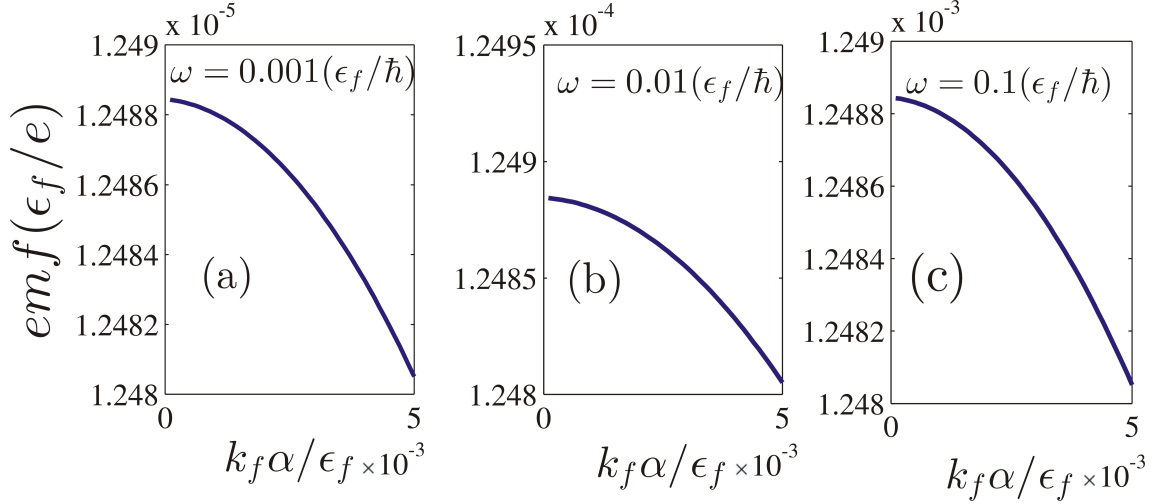


FIG. 6: The electromotive force induced in a Bloch type DW at different precession frequencies as a function of the Rashba coupling strength.

by a simple algebra it can be shown that

$$\begin{aligned}
 \Omega_{xt} &= \frac{1}{2} \det \begin{pmatrix} \partial\beta/\partial x & \partial \cos \gamma / \partial x \\ \partial\beta/\partial t & \partial \cos \gamma / \partial t \end{pmatrix} \\
 &= \frac{1}{2} \det \begin{pmatrix} \partial_x \theta & \partial_x \phi \\ \partial_t \theta & \partial_t \phi \end{pmatrix} \det \begin{pmatrix} \partial_\theta \beta & \partial_\theta \cos \gamma \\ \partial_\phi \beta & \partial_\phi \cos \gamma \end{pmatrix} \\
 &= \Omega_{\theta\phi} \det \begin{pmatrix} \partial\theta/\partial x & \partial\phi/\partial x \\ \partial\theta/\partial t & \partial\phi/\partial t \end{pmatrix}. \quad (34)
 \end{aligned}$$

Therefore electromotive force could not be generated when time and the special dependence of the effective field just appeared in one of the spherical angles. This means that in order to generate an electromotive force by a magnetic structure both of the spherical angles should vary in space and time.

VI. ELECTROMOTIVE FORCE DUE TO THE RIGID DOMAIN WALL MOTION

The localized spin texture of the DW configuration could be described by the following Hamiltonian

$$\begin{aligned}
 \mathcal{H}_{Loc} &= -J_{loc} \sum_{\langle i,j \rangle} \vec{n}(r_i) \cdot \vec{n}(r_j) \\
 &\quad - \sum_i (K_{\parallel} \vec{n}(r_i) \cdot \hat{e} - K_{\perp} \vec{n}(r_i) \cdot \hat{e}') \\
 &\quad - \sum_i \gamma \vec{n}_m \cdot \vec{n}(r_i) + \mathcal{V}_{pin} \quad (35)
 \end{aligned}$$

In which the first term describes the Heisenberg Hamiltonian of the first neighbor spins where J_{loc} denotes the

exchange coupling constant between the localized spins e denotes the easy axis while e' being the direction of the hard axis. K_{\parallel} , K_{\perp} stand for anisotropic constants for easy and hard axis respectively. $n(r_i)$ describes the direction of the localized spins as mentioned before. γ is the Zeeman splitting and \mathcal{V}_{pin} stands for pinning potential. The competition between the exchange and anisotropic couplings determines the DW width which is given by $d \sim \sqrt{K_{\parallel}/J_{loc}}$.

Meanwhile the dynamics of the local spins have been determined with the Landau and Lifshitz equation which could be expressed as

$$\frac{d\vec{n}(r_i, t)}{dt} = \gamma \vec{n}(r_i, t) \times \vec{n}_m + \alpha \vec{n}(r_i, t) \times \frac{d\vec{n}(r_i, t)}{dt}, \quad (36)$$

where α is the damping constant.

It can be inferred that the exchange interaction (H_{ex}) couples the dynamics of electron spins with background local magnetic moments.

DW motion can be considered as a successive spin switching of the local precessing moments as a result of the damping procedure. Local spins precessing about the direction of local effective field built up by the stray field and anisotropic magnetic couplings. When a static magnetic field is applied depending on the strengths of this field local spins start to precess about the direction of the new effective field which has been modified by the external magnetic field. When the magnetic field is higher than depinning field this precession ends when the precessing spin fall along the direction of effective field during the damping process. This was known as spin switching process.

Meanwhile moving DW itself could take place in different regimes. When the magnetic field is less than the Walker breakdown field²³ i.e. when the spin torque exerted as a result of the damping process is relatively high in comparison with the spin torque exerted by the magnetic field, DW moves actually in a shape preserved manner. In this case DW makes a rigid movement since the spin switching process takes place almost abruptly. Therefore rigid DW motion rests largely on how fast that the spin switching takes place. On the other hand when the magnetic field is higher than Walker breakdown field. DW will precess during its translational motion. As shown by Yang and et al for a moving DW without precession i.e for rigid DW motion there is no electromotive force in the system²². This could be demonstrated for both types of the DWs. In the absence of the precession, when the spin switching takes place abruptly, rigid DW motion could be described by the following profile $\phi = const, \theta(x, t) = \pi(x - v_D t)/a_m$ and $\phi(x, t) = (\pi/2) \tanh((x - v_D t)/d), \theta = const$ for Bloch and Néel type DWs respectively.

Using the Eq. 34 it can be inferred that electromotive force generated by DW motion identically vanishes for rigid translation of the DW in both of the mentioned configurations. This can be easily obtained if we consider that for either of the profiles given for the rigid

motion of the DW we have

$$\det \begin{pmatrix} \partial\theta/\partial x & \partial\phi/\partial x \\ \partial\theta/\partial t & \partial\phi/\partial t \end{pmatrix} = \frac{\partial(\theta, \phi)}{\partial(x, t)} = 0 \quad (37)$$

and therefore

$$\Omega_{xt} = 0 \quad (38)$$

VII. ELECTROMOTIVE FORCE GENERATED BY THE RIGID MOTION OF A DEFORMED DOMAIN WALL

If we consider the bulging effect in the DW it could be demonstrated that the rigid motion of the DW generates an effective electromotive force inside the system. DW bulging could be characterizes by a position dependent rotation axis, $\hat{n}_D(\vec{r})$ and the boundary curve of the DW where we have assumed that the DW rotation axis should be directed vertically to the DW boundary surface i.e. when the DW boundary has been specified by a surface described by $F(r_0) = c$ DW rotation axis is given by $\hat{n}_D(\vec{r}) = \nabla F/|\nabla F|$ at each point of the boundary curve. In the current case we have assumed a deformed Bloch type DW. If the direction of the local magnetization is upward at the left boundary of the DW then local direction of the magnetization could be obtained by the spin rotation operator as follows

$$\begin{aligned} \sigma \cdot \vec{n} &= R_{(\theta)}^\dagger \sigma_z R_{(\theta)} \\ &= \cos^2(\theta(X_D)/2) \sigma_z \\ &\quad + \sin^2(\theta(X_D)/2) \cos^2(\theta(X_D)/2) [\sigma \cdot \vec{n}_D, \sigma_z] \\ &\quad + \sin^2(\theta(X_D)/2) (\sigma \cdot \vec{n}_D) \sigma_z (\sigma \cdot \vec{n}), \end{aligned} \quad (39)$$

in which

$$\begin{aligned} R_{\theta(X_D)} &= \exp(-i\sigma \cdot \vec{n}_D(\vec{r})\theta(X_D)) \\ &= 1 \cos(\theta(X_D)/2) - i\sigma \cdot \vec{n}_D(\vec{r}) \sin(\theta(X_D)/2), \end{aligned} \quad (41)$$

R_{θ} is the spin rotation operator and $X_D(r, t) = \hat{n}_D(r) \cdot \vec{r}(t)$ is the projection of position vector along the direction of the DW rotation axis. Accordingly we can obtain

$$\begin{aligned} \sigma \cdot \vec{n} &= (\cos(\theta(X_D)) + 2n_{Dz}^2 \sin^2(\theta(X_D)/2)) \sigma_z \\ &\quad + (2n_{Dx}n_{Dz} \sin^2(\theta(X_D)/2) - n_{Dy} \sin(\theta(X_D))) \sigma_x \\ &\quad + (2n_{Dy}n_{Dz} \sin^2(\theta(X_D)/2) + n_{Dx} \sin(\theta(X_D))) \sigma_y. \end{aligned} \quad (42)$$

Therefore the unit vector of the local magnetization could be extracted as follows

$$\vec{n}(\vec{r}) = \begin{pmatrix} \cos(\theta(X_D)) + 2n_{Dz}^2 \sin^2(\theta(X_D)/2) \\ 2n_{Dx}n_{Dz} \sin^2(\theta(X_D)/2) - n_{Dy} \sin(\theta(X_D)) \\ 2n_{Dy}n_{Dz} \sin^2(\theta(X_D)/2) + n_{Dx} \sin(\theta(X_D)) \end{pmatrix}. \quad (43)$$

If we restrict ourself to the case of the two-dimensional

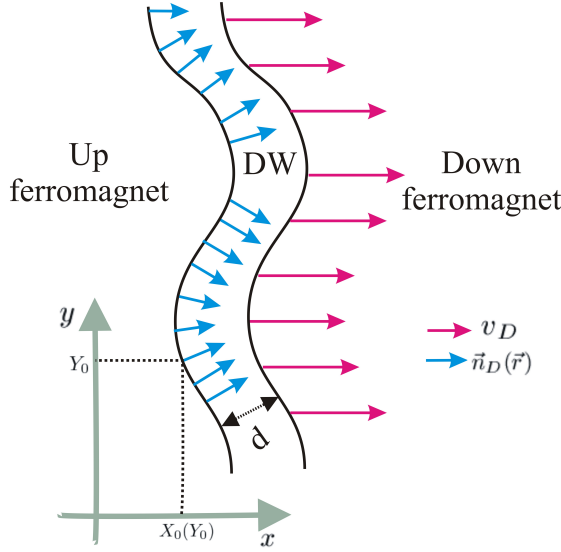


FIG. 7: A typical form of the deformed DW in the real space. DW has been placed between two oppositely directed magnetic domains. A Bloch-type DW has been considered in which the DW rotation axis located in the plane of the system. The bulging of the DW can be formulated if we consider that the DW rotation axis is always vertically oriented to the DW boundaries. n_D denotes the DW rotation axis while v_D indicates the speed of the DW and d is the DW width.

DWs i.e. when ($n_{Dz} = 0$) we obtain the simplest case of two dimensional bulging as follows

$$\vec{n}(\vec{r}) = -n_{Dy} \sin(\theta(X_D)) \hat{x} + n_{Dx} \sin(\theta(X_D)) \hat{y} + \cos(\theta(X_D)) \hat{z}. \quad (44)$$

DW width has been assumed to be locally constant during the DW rigid motion. The DW motion has been considered as a successive switching of the local spins that as mentioned before in the case of the rigid DW motion it was assumed that the spin switching time is very short and a localized spin switches abruptly without precession. Meanwhile it was assumed that the DW rigidly moves along the x axis. Since we can write $\phi(y) = \tan^{-1}(-n_{Dy}(y)/n_{Dx}(y)) = -\phi_D$ and $X_D(r, t) = \vec{n}_D \cdot \vec{r} = n_{Dx}(x - X_0(Y_0) - v_D t) + n_{Dy}(y - Y_0)$ where $X_0(Y_0)$ is the left boundary of the DW at the initial time. This curved boundary preserves its shape during the DW motion which sweeps and removes the downward ferromagnetic region (right region in Fig. 7) during the motion of the DW.

The space time Berry curve is given by

$$\begin{aligned} \Omega_{y,t} &= \Omega_{\theta\phi}(\partial_y \phi)(\partial_t \theta(X_D)) \\ &= \Omega_{\theta\phi} n_{Dx} v_D \partial_{X_D} \theta(X_D) (n_{Dx} \partial_y n_{Dy} - n_{Dy} \partial_y n_{Dx}). \end{aligned} \quad (45)$$

Since we can write $n_{Dx}^2 + n_{Dy}^2 = 1$, therefore $n_{Dx}(n_{Dx} \partial_y n_{Dy} - n_{Dy} \partial_y n_{Dx}) = \partial_y n_{Dy}$. Meanwhile in

the absence of the Rashba interaction i.e. when $\alpha = 0$ we have $\beta = \phi$ and $\cos \gamma = \cos \theta$ and therefore $\Omega_{\theta\phi} = 1/2 \sin(\theta)$. Accordingly

$$\Omega_{y,t} = \frac{\pi}{4d} \sin(\theta(X_D)) v_D \cosh^{-2}(X_D/d) \partial_y n_{Dy} \quad (46)$$

and similarly we can obtain

$$\Omega_{x,t} = \frac{\pi}{4d} \sin(\theta(X_D)) v_D \cosh^{-2}(X_D/d) \partial_x n_{Dy}. \quad (47)$$

Unlike the straight DWs in which the electromotive force could only generated as a result of the precession regardless of the DW motion, in the case of the deformed DWs we have shown that the rigid DW motion could produce an effective electromotive force.

VIII. CONCLUDING REMARKS

In the current study we have obtained different Berry curvatures of helimagnetic and DW spin structures for Bloch and Néel type configurations. Results of the current study shows that Rashba coupling plays a significant role in the Hall conductivity of Bloch-type magnetic configurations. As mentioned before k-space Berry curve measures the contribution of each k-state in the anomalous velocity. Results show that unlike the helimagnetic magnetic structure, in the DW magnetic configuration the contribution of different states in k-space Berry curve i.e. in the anomalous velocity is not symmetric in different directions of k-space. In the other words the direction in which the local spins are varying in the real space has the lower contribution in k-space Berry curve. Therefore the asymmetry of the real space has been reflected in the k-space Berry curve as well. Meanwhile when all of the local spins are coplanar k-space Berry curve identically vanishes and there is no contribution into the anomalous velocity and Hall conductivity. Coplanar spins even cannot contribute in the other Berry curves and the effects which could be measured by these curves.

As demonstrated in the previous studies in the current work we have shown that the spin precession in a pinned DW or helimagnetic structure generate an electromotive force. The electromotive identically vanishes in the absence of the precession in the other words the precession has been assumed the main factor in the generation of the electromotive force. Meanwhile we have shown that the electromotive force generated by the spin precession in Bloch type spin configurations decreases by increasing the Rashba coupling. Meanwhile in the current study it was shown that if we consider the bulging of the deformed DW electromotive force could be generated.

-
- ¹ C. H. Tsang, R. E. Fontana Jr, T. Lin, D. E. Heim, B. A. Gurney, and M. Williams, IBM journal of research and development **42**, 103 (1998).
 - ² C. Tsang, R. E. Fontana, T. Lin, D. E. Heim, V. S. Speriosu, B. A. Gurney, and M. L. Williams, Magnetics, IEEE Transactions on **30**, 3801 (1994).
 - ³ S. Solin, D. Hines, A. Rowe, J. Tsai, Y. A. Pashkin, S. Chung, N. Goel, and M. Santos, Applied Physics Letters **80**, 4012 (2002).
 - ⁴ J. Gregg, W. Allen, K. Ounadjela, M. Viret, M. Hehn, S. Thompson, and J. Coey, Physical review letters **77**, 1580 (1996).
 - ⁵ S. Lepadatu and Y. Xu, Physical review letters **92**, 127201 (2004).
 - ⁶ P. M. Levy and S. Zhang, Physical Review Letters **79**, 5110 (1997).
 - ⁷ U. Rüdiger, J. Yu, S. Zhang, A. D. Kent, and S. S. Parkin, Physical review letters **80**, 5639 (1998).
 - ⁸ B. Çetin and N. Giordano, physica status solidi (b) **241**, 2410 (2004).
 - ⁹ G. Tatara and H. Fukuyama, Physical review letters **78**, 3773 (1997).
 - ¹⁰ J. F. Gregg, W. Allen, K. Ounadjela, M. Viret, M. Hehn, S. M. Thompson, and J. M. D. Coey, Phys. Rev. Lett. **77**, 1580 (1996).
 - ¹¹ G. Tatara and H. Fukuyama, Phys. Rev. Lett. **78**, 3773 (1997).
 - ¹² R. P. van Gorkom, A. Brataas, and G. E. W. Bauer, Phys. Rev. Lett. **83**, 4401 (1999).
 - ¹³ .
 - ¹⁴ S. E. Barnes, J. Ieda, and S. Maekawa, Applied Physics Letters **89**, (2006).
 - ¹⁵ S. A. Yang, G. S. D. Beach, C. Knutson, D. Xiao, Q. Niu, M. Tsoi, and J. L. Erskine, Phys. Rev. Lett. **102**, 067201 (2009).
 - ¹⁶ S. E. Barnes and S. Maekawa, Phys. Rev. Lett. **98**, 246601 (2007).
 - ¹⁷ W. M. Saslow, Phys. Rev. B **76**, 184434 (2007).
 - ¹⁸ R. A. Duine, Phys. Rev. B **77**, 014409 (2008).
 - ¹⁹ R. A. Duine, Phys. Rev. B **79**, 014407 (2009).
 - ²⁰ Y. Tserkovnyak and M. Mecklenburg, Phys. Rev. B **77**, 134407 (2008).
 - ²¹ M. Stamenova, T. N. Todorov, and S. Sanvito, Phys. Rev. B **77**, 054439 (2008).
 - ²² S. A. Yang, G. S. D. Beach, C. Knutson, D. Xiao, Z. Zhang, M. Tsoi, Q. Niu, A. H. MacDonald, and J. L. Erskine, Phys. Rev. B **82**, 054410 (2010).
 - ²³ N. L. Schryer and L. R. Walker, J. Appl. Phys. **45**, 5406 (1974).
 - ²⁴ M. V. Berry, Proc. R. Soc. London Ser. A **392**, 45 (1984).
 - ²⁵ A. Tomita and R. Y. Chiao, Phys. Rev. Lett. **57**, 937 (1986).
 - ²⁶ K. Ohgushi, S. Murakami, and N. Nagaosa, Phys. Rev. B **62**, R6065 (2000).
 - ²⁷ Y. Taguchi, Y. Oohara, H. Yoshizawa, N. Nagaosa, and Y. Tokura, Science **291**, 2573 (2001).
 - ²⁸ R. Shindou and N. Nagaosa, Phys. Rev. Lett. **87**, 116801 (2001).
 - ²⁹ N. A. Sinitsyn, Journal of Physics: Condensed Matter **20**.
 - ³⁰ D. Xiao, W. Yao, and Q. Niu, Physical review letters **99**, 236809 (2007).
 - ³¹ T. Jungwirth, Q. Niu, and A. MacDonald, Physical review letters **88**, 207208 (2002).
 - ³² D. Ceresoli, T. Thonhauser, D. Vanderbilt, and R. Resta, Physical Review B **74**, 024408 (2006).
 - ³³ J. Shi, G. Vignale, D. Xiao, and Q. Niu, Physical review letters **99**, 197202 (2007).
 - ³⁴ D. J. Thouless, Phys. Rev. B **27**, 6083 (1983).
 - ³⁵ .
 - ³⁶ D. Xiao, M.-C. Chang, and Q. Niu, Rev. Mod. Phys. **82**, 1959 (2010).
 - ³⁷ D. M. Bird and A. R. Preston, Phys. Rev. Lett. **61**, 2863 (1988).
 - ³⁸ A. A. Belavin and A. M. Polyakov, JETP LETTERS **22**, 245 (1975).
 - ³⁹ D. Xiao, J. Shi, and Q. Niu, Phys. Rev. Lett. **95**, 137204 (2005).
 - ⁴⁰ V. Dugaev, J. Barnaś, J. Berakdar, V. Ivanov, W. Dobrowolski, and V. Mitin, Physical Review B **71**, 024430 (2005).